Final Report

Team 02: Robotic Delivery of Part Racks

MECH 462

April 15, 2022

Team Members:

Misha Kovarsky

Alex Marck

Geoffrey Baxter

Nick Thorpe

Spencer Tingle

Client: SigmaPoint Technologies Inc.

Faculty Advisor: Professor C. Mechefske

Course Instructor: Professor J. Sneep

Executive Summary

SigmaPoint, an Ontario based electronics manufacturer, is requesting a design solution to modernize their manufacturing product flow. The company prides themselves on their use of innovative “Industry 4.0” techniques and is interested in the automation of one of their internal value streams. This automated solution will carry parts in process across the SigmaPoint shop floor on metal wire racks, a process that is currently completed manually. The design was specified to be battery powered with enough torque to operate at normal walking speeds of approximately 5 km/hour under a total loading of 50 lbs. Collision detection and the ability for an operator initiated emergency stop is also essential.

The current proposed design is a contained unit attached to the bottom of the racks used at SigmaPoint. The control system, battery, and vision system are all contained and connected to the rack to maintain proper distance to the ground. The vision system will run on a Raspberry Pi micro controller. Yellow tape and QR codes will be used to guide the robot throughout the factory floor.

This document will outline the fabrication, assembly, testing of the final design. It will detail the components used, the included software, the steps taken to assemble the chassis and components, the testing criteria and performance assessment, as well as future recommendations for further improvements and implementation. Furthermore, problems encountered during the aforementioned process of fabrication, assembly, and testing are outlined in addition to their respective solutions. The finalized budget and economic analysis of the project is also included.

Table of Contents

List of Figures

1 Introduction

1.1 Background

SigmaPoint is an Ontario based company that focuses on the manufacturing of electronics, specifically custom printed circuit boards (PCBs). Originally a start-up in 1999, SigmaPoint has grown to producing a revenue of around 100 million dollars and employing over 350 people. They specialize in producing complex circuit boards for industry leading companies in the defense, aerospace, industrial, alternative energy, transportation, and medical markets. With the transition to offshore manufacturing, SigmaPoint has changed the game by providing competitive pricing to local electronics manufacturing. Focusing on customer relationships, faster turnaround, shorter lead time, innovation, and reduced shipping costs; they have proven that local companies can rival offshore suppliers.

With an innovated lean manufacturing process, SigmaPoint is proud of its execution and advancement in electronics manufacturing. To maintain their competitive advantage, continuous improvement of outdated processes is necessary. Transportation of products, kits, and parts to and from the assembly is one process that needs improvement and innovation. The current operation involves a push rack that transports thousands of delicate electronics every day. Operators do not always have time to transport these racks to their assembly station. This causes over cycle and loss of production. Automating the racks would highly benefit the manufacturing process and help push SigmaPoint towards implementing an "Industry 4.0" system.

1.2 Definition of Industry 4.0

As stated in their project outline document, SigmaPoint is committed to the adoption and development of "Industry 4.0" manufacturing techniques and technologies. Just as computerization transformed the manufacturing landscape during Industry 3.0, automation is once again revolutionizing the way goods are manufactured. The concept of Industry 4.0 is based on "smart" machines that can keep track of the product they are handling and communicate with the other machines that make up their production line. Automated inventory delivery is a great example of one of these intelligent automated systems in which the robot is aware of its inventory, surroundings, and objectives [1].

Another cornerstone of SigmaPoint's competitive manufacturing strategy is the use of "Lean Manufacturing" principles. In essence, lean manufacturing aims to remove as much waste within a manufacturing system as possible, in order to provide the best value for the customer. Many different parts of the manufacturing process can add waste, but some common contributors are wastage caused by overproduction, idle time, high number of quality failures, and inefficient product flow.

A common theme of lean manufacturing processes is the use of pull or demand-based production – in which manufacturing steps are completed on an as-needed basis. This often reduces the risk of overproduction and idle time [1].

2 Project Scope

This project aims to design an innovative solution that can automatically move existing part racks, such as the ones shown below in **Error! Not a valid bookmark self-reference.** 1 and have them travel along a fixed path in a manufacturing environment.

The client, SigmaPoint, wishes to improve production efficiency by automating the transportation of their parts within their factory. The scope of the project is quite limited to start off; the client wishes to see a proof-of-concept design before expanding the project to their entire production facility. Specifically, the first prototype will need to navigate the path shown below in **Error! Reference source not found..** In total, less than five carts will need to move between two predefined points in the plant. The carts are loaded with manufactured parts at point A by a production worker, before being transported to point B which is referred to as the "Finished Goods" area. Once the parts are unloaded at Point B, the carts will return to Point A following the same path. The carts will spend more than 50% of their time during a stationary shift at Point A. The exact time spent stationary and travelling between points is further discussed in Section 7.2. However, it is important to note that the times, as well as the travel distances will vary depending on the location of the rack within the plant. In total, the plant will utilize 20-to-40-part racks on any given day with various loading points throughout.

Figure 1. Existing parts rack used in SigmaPoint's production facility

Figure 2. Required path to be followed by the prototype automated part rack

Alongside the problem statement, SigmaPoint included a few constraints for the design itself. Most notably, the design is required to utilize a rechargeable power source that can last the duration of an entire shift (8 hours). Secondly, the motorization of the carts should not be mutually exclusive with manual operation. This means that the production workers should still be able to move the carts around by hand even with the motors installed. The device is required to provide enough torque to drive a 50lb rack. The racks will need to achieve a linear travel speed equal to walking speed (approximately 5km/h). Lastly, the

device needs to be safe from electrostatic discharge (ESD). This is because SigmaPoint primarily manufactures custom printed circuit boards (PCB's) that could be severely damaged if exposed to any form of static discharge.

The scope of this project is divided into two main sections: mechanical design and software/controls design.

The scope of the mechanical design of the project encompasses multiple components. Firstly, the team will design the mounting system for the mechatronic device, i.e., how the robot will attach itself to the existing part racks easily and efficiently. The mechanical team will also be responsible for selecting the appropriate motors to be able to move the part racks around at approximately 5km/h. Designs for the electrical circuit will also need to be completed, and an appropriate rechargeable power source will be selected. Lastly, the entire case for the robot and all its components falls under the scope of the mechanical team. This housing for the system will need to incorporate a way of dissipating any electro-static discharge (ESD) to the ESD-safe floor used at SigmaPoint's facility.

The scope of the software design of this project includes the navigational components and logic used by the robot. The team will choose the method of surroundings surveyance, the appropriate components for the chosen method, and the ideal mounting location of said components on the robot. Furthermore, the team will decide on the robot's positioning system for monitoring its location within the facility. Code development is included in each of these objectives as well. Within this code, the team will decide how the robot responds to either stationary or mobile obstacles, how the robot responds to directional guidance components, and how the robot responds to navigational checkpoints.

The scope of this report is to plan the economics, design plan, testing, and overall timeline of the next 8 weeks. A parts list and complete budget is submitted to provide a complete cost breakdown of every component required in our design. The solutions design, simulation, and assembly will be covered. Testing phase will be outlined in detail to insure reduced risk, improved safety, and proper evaluation of hour robotic solution. This will be covered for both mechanical and software testing. Lastly, a detailed summary of upcoming deliverables, assembly, testing schedule, and completion will be outlined in a ghant chart.

3 Problem Analysis

3.1 Problem Definition

Rack transportation adds to the workflow, and employees responsible for pushing racks may not deliver them immediately. Process downtime due to delayed part delivery is avoidable and negatively impacts productivity. In addition, a recent survey of the plant suggests that full racks can obstruct the pusher's visibility. Worker responses indicate it is common to experience near misses that could lead to safety incidents or damaged materials.

3.2 Objectives

The objective is to complete a working prototype that meets all the design constraints listed below. The solution must be safe, meet any workplace regulations, and meet SigmaPoint's requirements previously listed. Furthermore, the solution must easily integrate with SigmaPoint's current operations.

3.3 Constraints

- The rack must move at walking speed
- Manual operation of the rack must not be exclusive from its automation
- Must detect and avoid people and objects
- Must be capable of transporting a max load of 50lbs (Rack and load combined mass)

4 Design

4.1 Solid Works Model

The shape of the folded sheet metal body design can be seen in the render below. Note that there is plenty of room to store the motors, battery, microcontroller, and sensor suite all inside the chassis body while maintaining appropriate ground clearance.

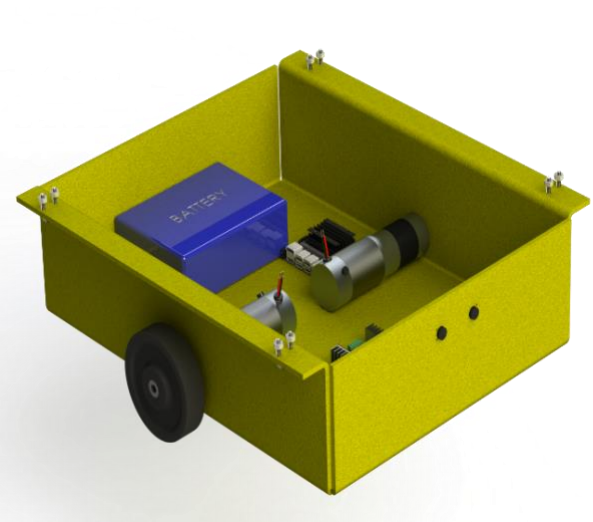

Figure 3. Render of the chassis body and its components

In the design shown above, the drive motors are directly mounted to the sides of the chassis, this reduces the risk of added complexity from separate parts and increases rigidity by reducing the number of mated components inside the chassis. The entire assembly fits underneath the product rack without increasing the birds-eye footprint of the system. This is in part a safety feature so that no part of the drive system is jutted out at foot level, presenting a tripping hazard for operators on the shop floor.

As stated above, rigidity of the chassis system is imperative for nominal operation of the autonomous rack system. While the chassis itself was designed for this constraint, the secure mounting to the product rack must also be considered since this too must be a rigid mechanical connection. The product rack geometry can be seen in the figure below.

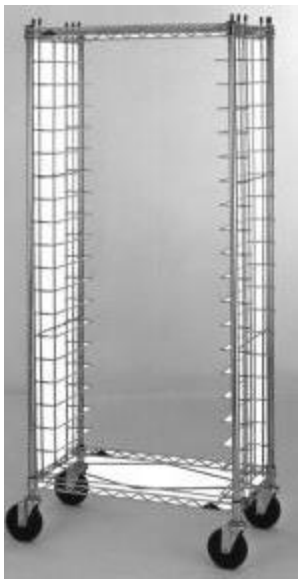

Figure 4. Steel wire frame part rack

This presents a non-trivial challenge since the product racks are composed of welded steel wire that do not provide many simple methods of attachment. Many different methods were considered, but it was found that the most simple and effective way to mount the chassis to these steel wires would be through the use of U-bolts fed through a flange on the top of the chassis and around the rack. As the locknuts on the U-bolt are tightened, the bolt cinches down onto the wire, pressing the chassis rigidly to the rack frame. A detailed view of this bolt mechanism can be seen below. Note that the flange would rest above the bottom wire of the product rack, with the U bolt slung underneath.

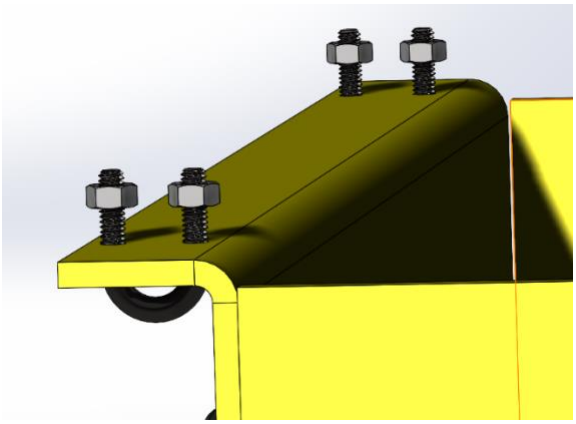

Figure 5. Rack mounting mechanism

While the U-bolt design does ensure a rigid connection between the drive system and the product rack, it also provides a simple method of dis-mounting if any maintenance needs to be done on the chassis system. If the locknuts are removed from the chassis frame, the entire system can be easily lifted away from the product rack.

Additional assembly views, as well as a complete drawing package is available in Appendix A – CAD Package.

4.2 Software

The software solution leverages computer-vision algorithms to aid its navigation. Navigation decisions fall into three categories: global navigation, local navigation, and collision avoidance. Global navigation includes understanding where the robot is located with respect to its destination. Local navigation involves making decisions to move through its immediate surroundings, such as staying within boundaries and moving in a straight path. Collision avoidance ensures the robot detects obstacles early and accurately to give the robot adequate time to stop. Each of these steps involves

4.2.1 Global Navigation

Connected Nodes

The software will use the *connected node* method to determine its relative position. This method simplifies map-based approaches by approximating each intersection as a 'node,' and the controller only stores information about which other nodes are adjacent. Each intersection has a checkpoint marker that contains data to inform the robot both of its current position and about the respective directions of adjacent nodes. Figure 6 below shows a visual depiction of how a factory layout is simplified to a connected node map.

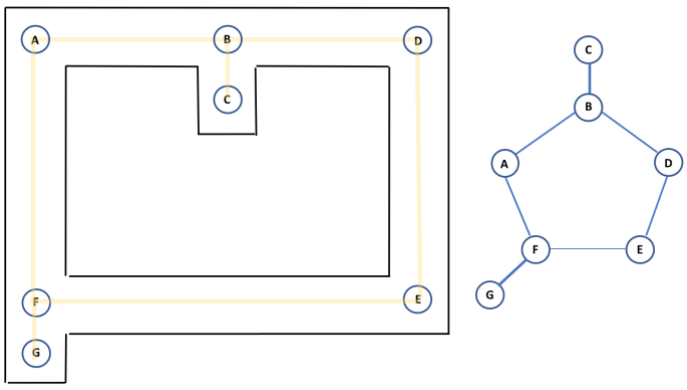

Figure 6: Example of how a factory map simplifies to a connected node map. Pictured left is a factory layout, and right is the corresponding node map. Note that the thickness of lines is used to represent connection weightings for some optimization algorithms.

QR Codes

QR Codes are used at each node to reorient the robot. Each QR code contains information about the current node's ID, as well as the IDs of its' adjacent nodes. The ZBar python library will be used to read the QR code, and the OpenCV library is used to identify and format the QR code.

Path Determining

The robot will check the information contained in the QR code against the internally stored node map to determine the required direction change based on the user inputs for start and end destinations. Once the QR code is read, the robot will move forward until it is at the center of the intersection. The robot will

identify that it is at the center of the intersection when the horizontal intersection line is no longer in its line of sight, roughly 20 cm away. It will move forward 20 cm with dead reckoning, then perform a rotation according to the instruction acquired at the QR code. It will then continue the straightaway routine.

4.2.2 Collision Detection

Detecting obstacles early and accurately gives the robot adequate time to stop and avoid collisions. The robot uses depth data acquired from the stereo camera, identifies objects, and returns the location of those objects. First, the cameras must be calibrated effectively to produce accurate depth images.

Camera Image Calibration

Before performing a stereo analysis on stereo images, the cameras must be calibrated such that the images are aligned in the same coordinate system. First, each camera must be calibrated to remove lens distortions. Next, the images must be rectified to reproject them on the same plane as depicted in Figure 7. OpenCV offers one-step procedures for each of these tasks, which involves using a printed checkerboard to automatically fit them to a shared plane. The rectification process was tested with the stereo-driving dataset, and the results are depicted in Figure 7.

Disparity Mapping

OpenCV offers the SGBM [10] (semi-global-block-matching) algorithm to generate disparity maps. It is an effective and quick method; however, the tuning process is involved. The SGBM method was tested on the stereo-driving dataset to create a depth map and is pictured in Figure 7 below.

Figure 7 : The results of applying the stereo mapping techniques to the stereo-driving dataset[12] The left and right images are overlayed before processing [left], then the frames are undistorted and rectified [center]. The disparities are calculated and transformed to a depth map [right]. Object bounding boxes are overlayed to highlight blob detection in the depth map.

Blob Detection

The blob detection method is used to detect regions of the depth map that significantly contrast their surroundings. The depth map will identify features on the floor plane, such as the guideline. To account for plane features that may be mistaken as blobs, the camera is placed such that its optical center does not intersect with the floor plane (i.e. collinear to the ground). If the center of the camera's vision cannot see the floor, it can be assumed that all features in the top half of the depth map will not contain features from the ground plane. Very small objects that are shorter than the camera height may not be identified in this solution, therefore it is critical that the camera placement is low.

4.2.3 Local Navigation

The robot will use yellow tape as a guide rail to navigate between nodes. The yellow tape provides a strong visual contrast against the surrounding environment to allow for reliable line detection.

Line Identification

The image is thresholded to isolate the yellow tape from the surroundings. A Hough transformation was initially considered to identify the line; however, the results were not reliable enough for autonomous navigation as described in section 5. Instead, a sliding window technique based on Automatic Addison's method was used.

Birds Eye View

Before processing, the lane lines angles towards the center of the frame, known as the vanishing point. To get a cartesian representation of the ground, OpenCV's warped perspective method is used to achieve a birds eye view of the floor. A GUI was created to enable the user to select the area of observation.

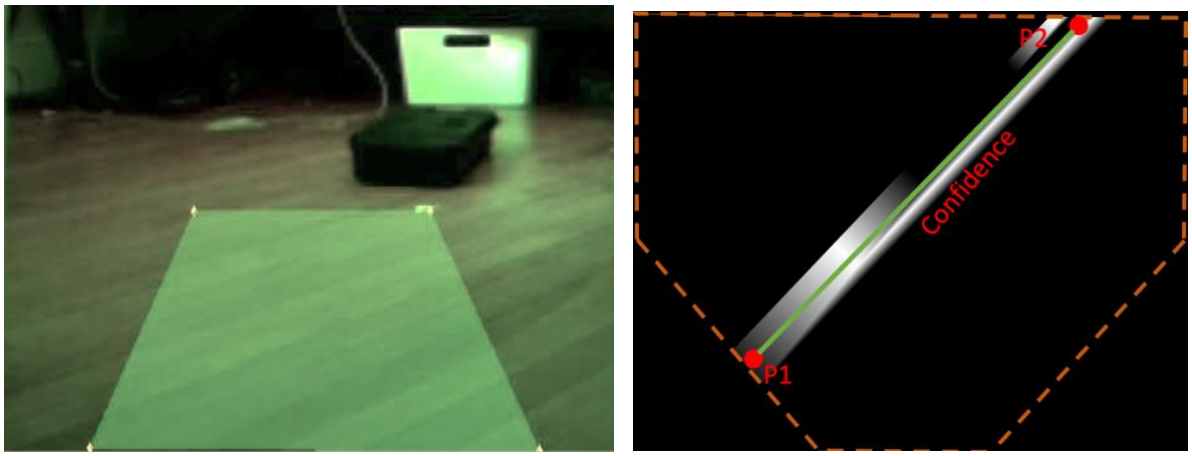

Figure 8: [left] GUI to select Region of Interest, and [right] transformed result. Images are discoloured green due to RAW format. P1 and P2 are the coordinates of the top and bottom of the line.

Thresholding

The new perspective of the floor is next thresholded to isolate the line pixels from the floor. A GUI was created to sample HSV values from the line, then another GUI was implemented for the user to adjust the upper and lower limits of the image.

Sliding Windows

A histogram threshold is performed to identify some starting coordinate of the line. 20 windows of height $h_{frame}/20$ are used to identify adjacent line pixels. A window observed directly above the starting window, centered at the highest histogram value of the previous window. This process is iterated over the entire height of the window. A line is then fit through the windows.

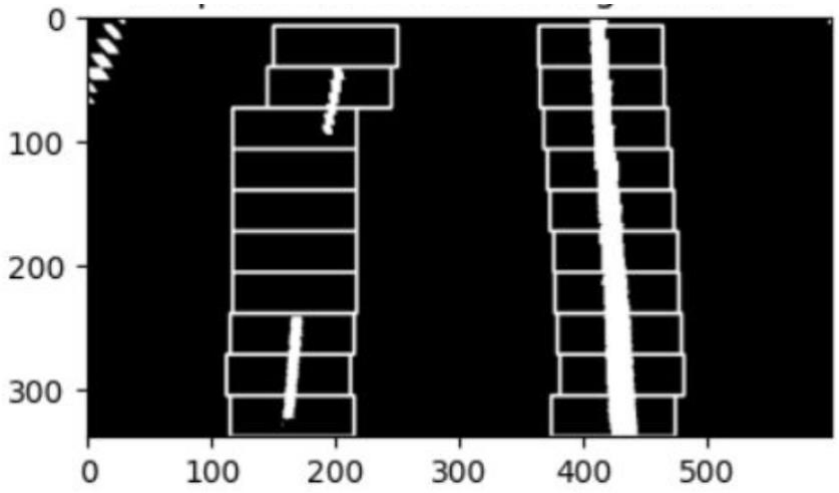

The confidence of a window is the number of pixels in a window divided by the minimum number of pixels for a window to be valid. The line confidence is the average of all windows in a line. This confidence estimate, along with the top and bottom coordinates of the line returned to the decision making unit (DMU).

Straightaways

Along straight paths between checkpoints, the robot must check for obstacles, follow the line, and identify upcoming intersections. To maintain course, the computer uses a force-vector approach, where the attractive vectors encourage the robot to move in the correct direction, while repulsive forces slow the robot down from potential obstacles or walls.

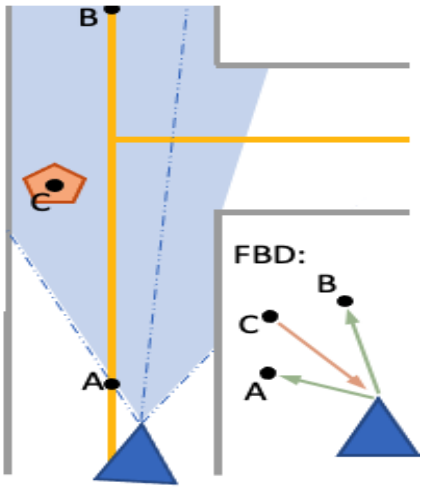

Figure 9: Visual example of the force vector field. Point A is the bottom of the line, point B is the top of the line, and point C is an obstacle. The bottom right corner illustrates the resulting free body diagram. Blue

First the program reads the most recent camera frame and processes it to identify any objects and returns the coordinates of the nearest one. Simultaneously, the line identification process returns the coordinates of the top and bottom of the vertical line. If a horizontal line is also detected, it will return the coordinates of the intersection. The coordinate of the top of the line, bottom of the line, and nearest objects are used to compute their respective force vector with a simplified version of newton's law of universal gravitation.

$$F_{12} = G\frac{m_1 m_2}{r^2} \qquad (1)$$

where G is replaced with a calibrated weight that is unique for each object. Appropriate weights will be calibrated during testing. A visual representation of this technique is pictured in **Error! Reference source not found.**. Masses will be set to one as the main scaling in this equation is from the weighted constant G.

Movement Decisions

The force vectors will be resolved into x and y components and used as error in the PID controller. The max top speed of the left and right motors will be represented as $delta_{max}$. Initially the left and right wheel speeds $delta_L$ and $delta_R$ will equal $delta_{max}$, and then are adjusted according to the error due to horizontal force. Next, the error due vertical (forward facing) forces is used to scale these deltas further. The control diagram for this process is pictured in Figure 10 below.

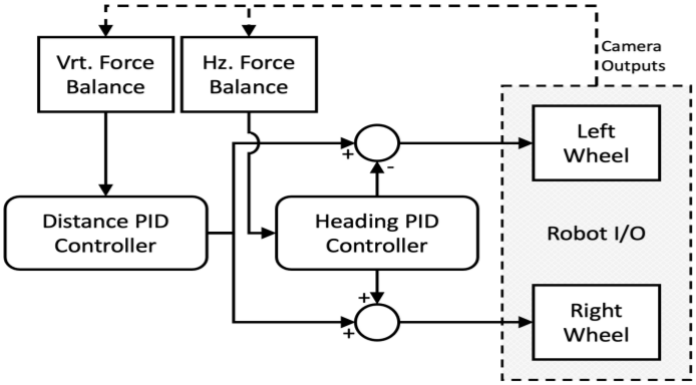

Figure 10: Preliminary control diagram for the PID Controller on straightaways

4.3 Assembly

Once the aluminum chassis has been fabricated to the proper dimensions, the assembly process can begin. Figure 3 outlines the main components that make up the robotic delivery of parts racks solution. First, the two motors will be mounted to the side of the chassis walls using four M5 bolts per motor. Then, the wheels will be attached to the motor using another M5 bolt. The stereo depth camera will be mounted to the front of the chassis using two M5 Bolts. Motor driver and micro controller will be attached in the chassis using Velcro to allow ease of removal for programing. The battery will be attached to the chassis using Velcro to allow for ease of battery swap. To mount the chassis to the steel wires on the rack, U-bolts will be fed through a flange on the top of the chassis and around the rack. This provides a simple method of dis-mounting if any maintenance needs to be done on the chassis system. If the locknuts are removed from the chassis frame, the entire system can be easily lifted away from the product rack. Lastly, wires will be installed from the battery to the motor driver, micro controller, and both motors. Wires with a 18 AWG copper wiring.

4.4 Final Design (Misha)

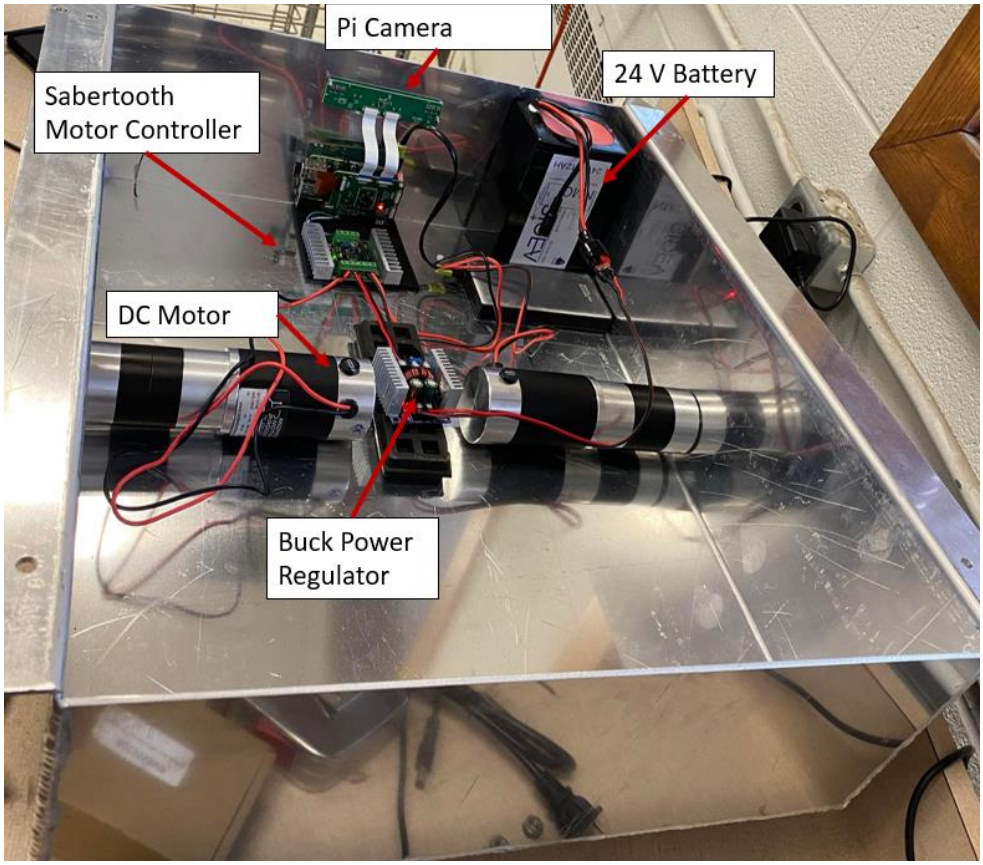

Figure 11: Labelled Inner Chassis Wiring

5 Engineering Tools and Evaluation of Solution

5.1 FEA

A simple SOLIDWORKS linear finite element study was completed on the aluminum chassis to ensure a 1/8" sheet thickness was appropriate. Using a 2 kN load applied on the motor mount face of the chassis, the displacement field was observed to verify no large-scale deformation occurs. Note that 2 kN is a load significantly higher than the expected maximum force to be experienced by the chassis. The displacement field yielded from this study can be seen in Figure 12 on the following page.

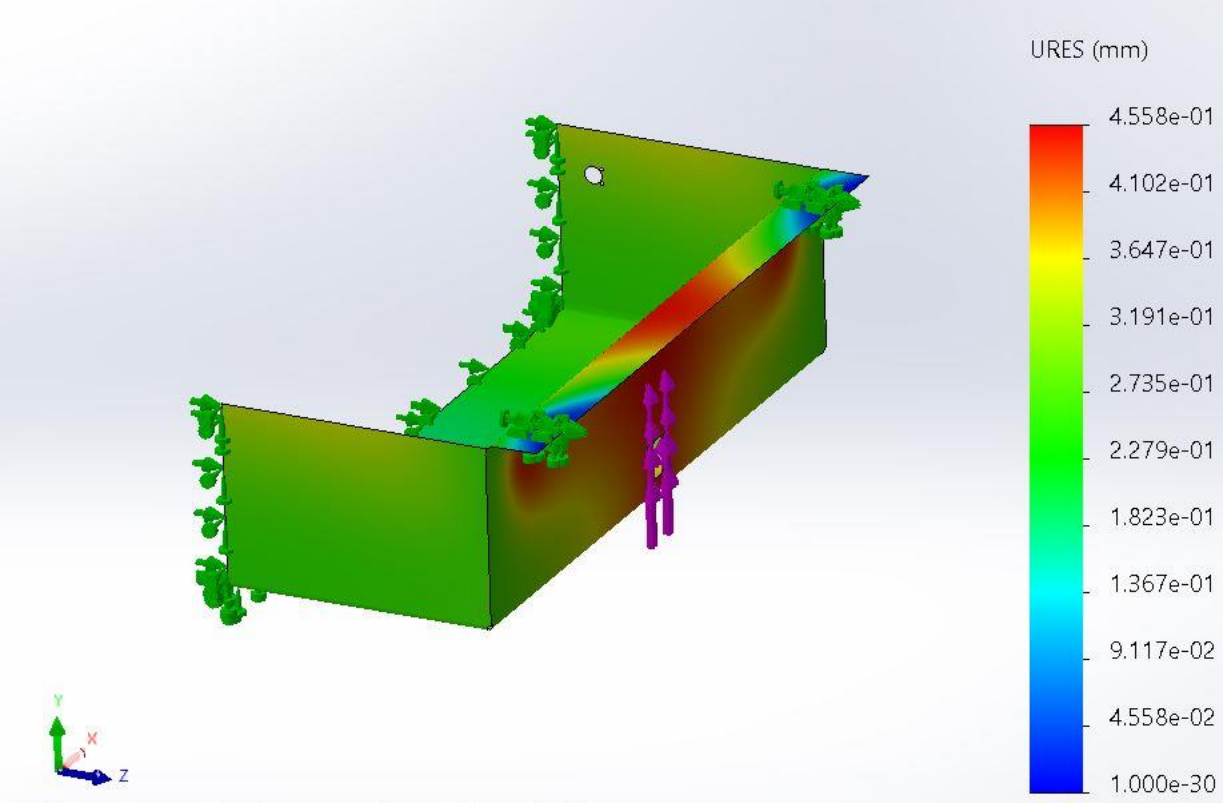

Figure 12: Linear Study Displacement of 1/8" Sheet Chassis

5.2 Fabrication Process

While many manufacturing techniques were considered for the chassis design, such as single body milling, welding, or even 3d printing – it was clear that the use of folded sheet metal was the optimal process to be used for this design. Folded and welded sheet aluminum assemblies are an incredibly cost-effective option for manufacturing parts of simple to intermediate complexity as two- and three-dimensions structures can be fabricated from a flat sheet of stock material through the use of laser or waterjet cutting and folding. This is a stark contrast from a manufacturing process such as milling wherein all the negative space in a part must be cut away, often resulting in a significant amount of original stock material being wasted. Sheet metal structures can still be very rigid, especially if the miter edges of a folded shape are welded together. The rigidity of the sheet structure can also be tuned by changing the thickness of the stock material (known as gauge).

A historical disadvantage of the folded sheet metal process is the need to account for bend radii; since all metals cannot bend at a perfect 90 degree, there is some amount sweeping radius as the material folds up. These bend radii can be seen below in Figure 8. This often meant that folded parts would be slightly oversized that the original spec, causing poor tolerances when compared to other traditional manufacturing processes like milling. With the advent of accurate material gauge table data from significant physical material testing, as well as electronic accounting using CAD software such as SOLIDWORKS, these bend radii can be perfectly accounted for to ensure appropriate dimensional tolerances of the final part.

An oft-overlooked step of the manufacturing process is surface finishing. Abrasions and dents on the surface of a metal part can significantly reduce the material's yield stress criterion and cause unplanned failure. There are many surfaces finishing options for aluminum that can increase the durability and effectiveness of a part. These include anodizing, powder coating, polishing, liquid painting – and many others. While each option has their own pros and cons, powder coating was chosen due to the significant durability of the finish, which will ensure longevity even in a factory floor environment, and its cost effectiveness. The powder coasting process involves using electrostatic discharge on a metal surface in order to attract a sprayed powdered paint before using a heat treatment to permanently bake the paint on the surface. Some powder coating treatments also have the benefit of being ESD safe, reducing the risk of static shock to important electronic equipment. Powder coats can come in various colors; yellow was chosen for the chassis body to allow for easy identification on the shop floor, increasing safety for operators that are working nearby the rack systems during autonomous operation. Note that the ESD safe coating is not included in the prototype budget, but it is recommended for the final non-prototype design.

Due to an unfortunate miscommunication involving the proper part number for the wire rack to be supplied to the team for testing, the chassis was built to fit a larger rack frame. The figure supplied below shows the supplied rack (left) and the rack that the chassis has been designed to accommodate.

Figure 13: Supplied Wire Racks

Due to this error, a custom wooden test rack frame was built to complete the planned suite of system testing. This simple rig, consisting of a ½ " plywood mounting plate, three caster wheels and a 2x2 frame structure was used as a replacement for all outlined testing. An image of the testing rack can be seen below. While this was an unfortunate setback, this event demonstrates the adaptability and tenacity of

the team. Once this dimensional error was noticed, the new test rack was designed and fabricated in less than a 24 hour period.

1.1 *Figure 14: Test Rack Assembly*

5.3 Obstacle Avoidance

The original plan to use OpenCV's StereoSGBM algorithm to produce depth maps was limited by current microprocessor shortage. The StereoSGBM algorithm was deployed on the Raspberry Pi, however its processing power allowed a framerate of only 1-2 FPS. In the spirit of working towards a proof-of-concept design, two alternative solutions were developed. The first option was to compromise depth map quality to increase sampling speed by using the lower quality stereo-matching algorithm, StereoBM. The second option was to forego real-time depth mapping and evaluate the algorithm on post-processed video in preparation for a higher quality microprocessor in the future.

Before the StereoBM solution was implemented, three criterion were identified to assess the quality of the stereo-matching algorithm. First, the algorithm must produce depth-maps at an adequate framerate. The lag time between the time that a frame is captured and the depth map is processed, t_{lag}, must allow enough time for the robot to slow down from walking speed. The team identified 1m as an acceptable stopping distance. This constraint is expressed as

$$1\ m \leq\ d_{stop,min} + t_{lag} * V_{max}$$

Where $d_{stop,min}$ is the the distance covered during the maximum safest acceleration to avoid tipping. For a maximum walking speed of 1.5 m/s, the $d_{stop,min}$ is 0.385 m, thus t_{lag} must be less than 0.41 s. Given a safety factor of 2, the framerate must be greater than 5 FPS. The StereoBM algorithm was able to produce a framerate of 15 FPS, which is more than adequate for this constraint.

The second two criterion were based on the quality of depth maps. First and foremost, the depth map must be be free of bad speckles. Bad speckles are regions where the disparity map produces estimates that are too close. When low quality algorithms like StereoBM produce estimates that a cluster of pixels are too close, these estimates could cause false collision warnings and lead to large uncertainty in movement. The StereoBM algorithm produced speckles as highlighted as red speckles in the figure below. Next, the algorithm must be able to produce depth estimates with enough quality to properly detect potential collisions. This is difficult to quantify, however the StereoBM algorithm was able to produce depth maps with surprising quality.

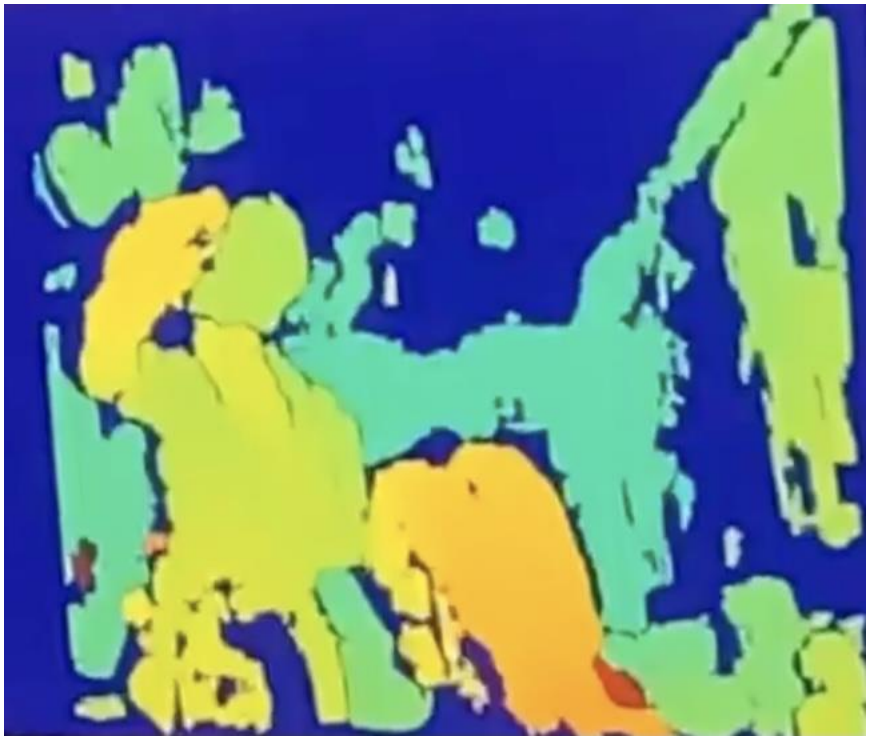

Figure 15: Depth map from stereo camera using StereoBM algorithm. Note the red speckles that indicate false readings.

In the end, StereoBM was not feasible to deploy for autonomous navigation. With more time to calibrate and post-process, a solution with StereoBM may have been feasible, however the false speckle problem presents a significant obstacle to this algorithm.

5.4 Testing

5.4.1 Line Following and QR Codes

Due to the iterative nature of developing robotic software, line following and QR reading were continually tested and changed during development. This development occurred in three parts: line identification, line following, and QR/intersection handling.

Line Identification

Line identification is the most fundamental component of navigation; without a high-quality estimate of the line, the robot may veer off course. The testing criteria for the line identification algorithm are in the following table.

Table 1 – Line identification algorithm evaluations. Each criteria is evaluated on a scale of 5.

Criteria	***Hough Line***	***Sliding Windows Technique***
Accuracy of line	*2*	*4*
Performance at steep angles	*4*	*3*
Performance in different light levels	*3*	*4*
Performance on a dirty line	*2*	*4*
Behavior around similar colored objects	*1*	*4*
Ability to detect the line through discontinuities	*2*	*5*
Performance at intersections	*2*	*4*

Initially, the Hough transform method was used for this, however it performed poorly in all tasks. This method identifies lines at color changes, and due to the rough result after thresholding, the line was often inaccurate or picked up bad values.

When the sliding windows technique was used, the line was consistently detected at head-on situations. It performed well in bright conditions, however the difference in lighting due to time of day lead to worse performance at the end of the line. In lower light conditions, the first 50% of the line was identified. The effects of this are detailed in the line following section. Several small pieces of tape were placed in the peripheral of the cameras vision. These small pieces of tape had little effect on the line's performance. There were instances where at intersections,

the line jumped to an intersecting line when the robot was oriented at an angle. The algorithm was extremely flexible to large gaps in the line, and was able to fit the line when two pieces of paper were used to cover the middle of the line. It's performance on a dirty line performed above expectations, as the line was not cleaned for several days and there was no drop in performance. The only situation where the line fit poorly was when the robot was placed perpendicular to a line, however it was able to reliably detect the line at a 75º rotation.

Line Following

Once the line identification algorithm performed adequately, the line following algorithm was developed with several behavioral tests in mind.

Table 2 – Performance criteria for line following performance. All items are discounted one point since the robot has not been tested at full speed.

Criteria	**Performance**
Starting position at an angle	3/5
Starting position without view of the line	N/A
Starting position parallel but off-centre of the line	3/5
The above conditions, close to the end of a line.	2/5
Following a discontinuous line	4/5
Stopping at the end of a line	4/5
Following a line in low light	2/5

The performance in these tasks were assessed based on repeatability and, speed. Early iterations of the line-following logic performed poorly, however the robot eventually passed all of these tasks in repeatability. The limitations of the design space did not enable testing faster speeds, and there is considerable work left to achieve acceptable speeds.

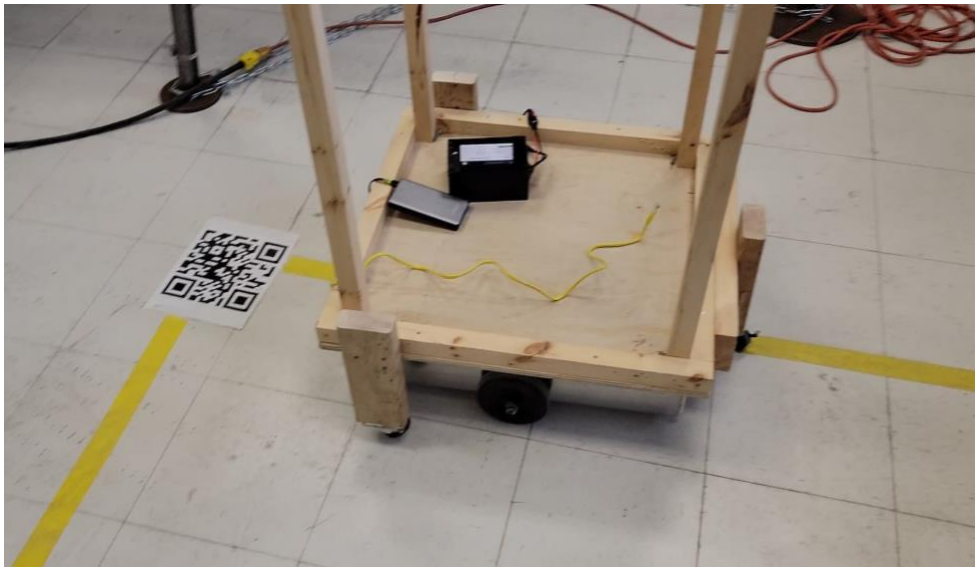

Figure 16: Snippet of System in the Middle of Line Following

QR and Intersection Handling

The final element of navigation that was tested was the handling of intersections. The QR scanning algorithm was tested to determine the following.

Table 3 – Performance of identifying a QR code at an intersection. All are scored on a scale of 5.

Criteria	**Performance**
Performance on an angle	3/5
Performance in low light	N/A
Maximum distance to see QR code	2/5
Consistency when approaching at an angle	3/5
Dirty QR code	5/5

The QR code scanning was robust and was able to identify the QR code in all tests without fail. The maximum distance to see the QR code was roughly 60cm away, however due to the limited area of the birds eye view, the viewing region is only between 30cm-60cm away. Further, this was not tested at full walking speed.

Once the QR code was working properly, the intersection routine was developed. For the testing, the QR code only contained one of three commands: left, right or straight. Because the intersection routine uses dead-reckoning, the robot was primarily tested by its performance on a dirty floor, and its performance at low battery.

Performance on a dirty floor had little effect on dead-reckoning distance or turning angle, since the robot was tested at very low speeds. It is feasible that more extreme speeds or conditions could lead to slippage, however for now the slow speed is a reasonable compromise. The performance on a depleted battery was more concerning since the turning speed is highly

dependent on the supplied voltage. The solution to this is higher turn speeds, however this conflicts with the dirty-floor problem.

5.4.2 Load support and Braking

Unfortunately, due to technical difficulties, no tests were able to be run for the acceleration, braking, and load capacity of the system. However, this paper will outline the testing plan, the goals of the tests, and recommendations for further testing in the future.

5.4.3 FEA Verification

The maximum displacement at full loading was modeled to be approximately 0.46 mm as described in the Finite Element Analysis section 5.1. With the final chassis loaded at maximum capacity, there was a displacement of significantly less than one millimetre – this was the expected result and the FEA conducted in semester one was successfully verified.

Acceleration and Speed

One of the primary requirements of the system as outlined in the project description was that the machine drive at "walking speed", or approximately 5km/h. In order to test this, the system would have been timed driving along a line of known length. This would be tested at a series of different loadings, from an empty rack, up to the necessary 50 lbs, and then beyond to test the maximum capabilities of the system.

Braking Time

In order to offer a safe system, the rack needs to be able to come to a full stop fast enough to avoid a collision. As such, a test would be run where the rack would drive along side a measure, either a tape measure, or a set of stripes of known size. The rack would be brought to a full stop from moving, and the braking time would be recorded. This test would be run with an unloaded rack, and a series of loadings up to the necessary 50lbs. As well, when testing with an official floor model rack, the tests should be run again with the weight suspended near the top of the rack so as to ensure the rack wouldn't tip over or drop materials upon sudden stoppage.

5.4.4 Battery Capability

Originally the scope included that the robot must be able to last an 8 hour shift between charges. This would allow for battery swap in between shifts. After discussing with SigmaPoint, we agreed it made more sense to purchase a smaller battery for testing. However, the team decided to test the battery specifications to provide information on the battery required to last an eight hour shift

As previously discussed in other reports, calculations were made to spec a battery that would support a full shift. It was discovered that a battery with approximately 37 Amp hours would be required. To test the accuracy of these calculations, we elevated the robot and ran the motors at maximum capabilities with a fully charged battery. A stopwatch was used to measure the amount of time until the battery ran out of charge. It took approximately 87 minutes to drain the battery. Given that SigmaPoint estimated the robot would operate about 4 hours in a shift and the battery used had 12 Amp hours of charge; a 33.1 Amp hour battery would be the minimum requirement to support a shift. This is an estimate of the battery sized necessary and testing on the plant floor would be required to determine the actual battery usage. The stress of stopping, starting, and rapped breaking may have a greater impact on battery usage. Also, the amount of time the robot will be operated in a given shift is an estimate made by SigmaPoint. Therefore, multiple tests during an 8 hour shift would need to be conducted to determine the actual battery size needed.

6 Economics

The economic argument for automation of parts rack delivery is simple. The useful labor time taken away each shift from operators moving the rack could be directly put back into other more complicated and expensive tasks if the movement were to be automated. The build and implementation costs of this relatively simple tasks is miniscule in comparison to the costs of an operator's time over the course of months or years.

As described in depth in section 7.0 Final Design Description, all facets of the overall design solution factored cost effectiveness as a key factor during the design phase. Parts were selected or designed in order to meet all functional parameters while minimizing cost to the client. A Bill of Materials can be seen below which comprises are parts required for a single automated rack system. The numbered items in the table also correspond to the assembly Bill of Materials Diagram available in Appendix D – CAD Package for visual reference.

The bulk of the costs of this design come from machining time and motor procurement. As described in depth above, while the costs are still significant for a cut and welded sheet metal body, it remains the most effective solution to the user requirements given. Any other form of traditional manufacturing would have increased costs to an infeasible level. As for the motors, the proven durability and reliability of Midwest Motion DC motors makes the upfront costs unquestionably worthwhile when considering the maintenance and down-time costs associated with a less reliable product. The microcontrollers and other electronic components make up a much smaller portion of the total budget. This advent of low-cost electronics available even to enthusiasts has significantly impacted the feasibility of projects like these, wherein even two decades ago, the bulk and heft of an equivalent PLC based system would have proven this design impossible.

Note that most costs are based on United States Dollars and converted to Canadian Dollars for ease of reference. This bill does not consider tax or associated shipping and duty costs and assumes an exchange rate of 1.26 CAD per United States Dollar.

No.	Part No.	Description	Supplier	Shipping Time	Site Link/Contact	Qty.	Pkg.	Cost ($USD)	Cost ($CAD)
Purchased Materials									
1	CH-001	Aluminum Chassis Stock	MetalPros	2-3 Days	https://quote.metalpros.com/?search=&shape=	1	1	-	225.00
2	2936T31	Galvanized Steel U Bolt	McMaster-Carr	2-3 Days	https://www.mcmaster.com/2936T31/	4	5	4.15	5.27
3	d22376gp2	DC Gearmotor	Midwest Motion	3-5 Days	https://midwestmotion.com/products/brgp/2	2	422	844	1071.88
4	2328T78	ESD Safe Rubber Wheel	McMaster-Carr	2-3 Days	https://www.mcmaster.com/d22376gp2/	2	1	23.58	29.95
5	405867542	Battery Pack	DH Gate	1-3 weeks	https://www.dhgate.com/product/rechargeabl	1	1	-	562.69
7	RB-Dim-42	SABERTOOTH DUAL 12A MOTOR DRIVER	RobotShop	5-10 days	https://www.robotshop.com/ca/en/sabertoot	1	1		99.94
8	-	Push Button	Amazon	6 Days	https://www.amazon.ca/Electop-Power-Buttor	1	1	-	12.27
9	-	Camera Extension Cables	Newegg	2-3 weeks	https://www.newegg.ca/p/169-001S-00329?It	2	1	-	10.45
10	-	Raspberry Pi 4 Extreme Kit	Amazon	7-14 bus. days	https://www.amazon.ca/CanaKit-Raspberry-Pi-	1	1	-	255.16
11	-	Arducam 8MP Stereo Camera Kit	Uctronics	7-4 bus. days	https://www.arducam.com/product/synchron	1	1	-	159.99
12	92290A232	316 Stainless Steel Socket Head Screw M5 x 0.8 mm Thread, 16 mm Long	McMaster-Carr	2-3 Days	https://www.mcmaster.com/92290A232/	1	25	11.39	14.35
13	-	Micro USB to USB C - 5V 3A - 25 cm	Amazon	6 Days	https://www.amazon.ca/dp/B07T2BZSR9/ref=s	1	1	-	12.42
14	-	Floor Marking Tape - YELLOW - 33 Yds	Amazon	6 Days	https://www.amazon.ca/gp/product/B08TV29	1	1	-	15.81
15	9697T2	18 AWG electrical wire	McMaster-Carr	2-3 Days	https://www.mcmaster.com/9697T2/	1	1	0.39	0.49
16	3051T11	Zinc Plated Pipe Strapping	McMaster-Carr	2-3 Days	https://www.mcmaster.com/3051T11/	1	1	4.79	6.08
Labour									
17	CH-001	Aluminum Chassis Manufacturing	McLaughlin Shop	1-2 Days Shop Time	andrew.bryson@queensu.ca	1	1	-	250.00
Contingency									200
Total									**2931.76**

Figure 17: Total project budget

Note the contingency allotment of $200 CAD was included to cover any unforeseen purchases. The final cost of the design solution was in line with the expected breakdown as shown in the budget above. The contingency budget was used to purchase the lumber and caster wheels for the test rack as described in section 4.4, as well as a buck power regulator as described in section 5.4.2. We were able to complete all required design and testing without the need for any extraneous purchases that would have come as a surprise to the client.

7 Project Management

Organised and effective project management skills were crucial to the completion of our capstone solution. After receiving all the parts from our budget list, important tasks were spear headed by different members of the group. The remaining team members support the leader of each task. The main assignments were assembly of the robot, software and debugging, and each capability test. To ensure the solution was completed on time, a strict schedule was followed. Upon receiving all the parts in week 9, the assembly process began. The process was finished by the start of week 10 so that the programing and debugging phase could begin. Once the line following and QR code reading worked reliably, we began the testing phase in week 12. The team worked extremely hard to maintain organization and deliver a working prototype.

Throughout the completion of the robotic delivery of part racks solution, the team encountered multiple issues the required significant problem solving and project management skills. Overcoming these problems showed that our team is flexible and motivated to tackle any obstacles. Table 4: Obstacles encountered and their solutions below displays the main difficult challenges faced throughout the semester and how the team solved each issue.

Table 4: Obstacles encountered and their solutions

Obstacles	Solution
The Jetson micro controller needed for our solution is out of stock for upwards of two years. This is due to the microchip shortage. Our next best option was to purchase a Rasberry Pi micro controller. Unfortunately, this controller does not provide enough CPU power for object detection and avoidance in real time.	Using the proper software, we were able to post process video collected by our camera and micro controller set up. This software can simulate object detection and be implemented into the design if a jetson controller is acquired.
Unfortunately, SigmaPoint provided us with the wrong rack part number. Therefore our chassis was designed to rigidly fit on the wrong rack.	A wooden rack was built so that we could still conduct the proper testing required.
The 24V battery purchased has an output voltage of 29.2V. The 24V motor driver purchased can only support up to 28.2V making it incompatible with the battery when directly connected.	After doing research and making multiple calls, a solution was found. We implemented a buck converter between the battery and motor driver. This dropped the voltage to an acceptable

	level that the motor driver could handle.
In the original design, we had planned to use the 5V output on the motor driver to supply the micro controller with power (as advertised). Unfortunately, this output could not provide enough amps for the micro controller to run at full strength.	We implemented a small power pack to supply the micro controller with enough amperage. The power pack was then connected to the 5V output on the motor controller to be charged by the main battery.

8 Future Work

Future work will be involved to bring the robotic delivery of parts rack solution from prototype to finished product. As previously discussed, a Jetson micro controller is needed to do obstacle avoidance in real time. This is crucial to ensure safety on the plant floor and guarantee the robot does not crash into any obstacles. Since the chassis was designed for a different rack, SignaPoint will need to provide the proper dimensions so that a new chassis can be manufactured. The chassis can also be optimized further to reduce the amount of required sheet metal. There is a significant amount of extra room inside the chassis body. If the robot is to be mass produced for many racks, an optimized design reducing material would provide a lot of cost savings. The chassis could be redesigned to more optimize battery swap between shifts. Our scope for the initial prototype was also reduced to traveling between two areas on the plant floor. In reality, the system will be traveling to multiple stations along each assembly line. Improving the program to optimize travel between multiple locations would be a difficult task and would further improve the robot. Lastly, a user interface could be designed for the robot. This could allow the operator to choose the next location the robot will travel to deliver or restock microchip components.

Marr, B. (2018, September 2). *What is Industry 4.0? Here's A Super Easy Explanation For Anyone*. (Forbes) Retrieved October 3, 2021, from https://www.forbes.com/sites/bernardmarr/2018/09/02/what-is-industry-4-0-heres-a-super-easy-explanation-for-anyone/?sh=6d99db469788

ROBOTIQ. (n.d.). *RobotIQ.* Retrieved February 02, 2022, from https://blog.robotiq.com/hubfs/eBooks/ebook-ISOTS15066-Explained.pdf?hsLang=en-ca

Appendix A – CAD Package

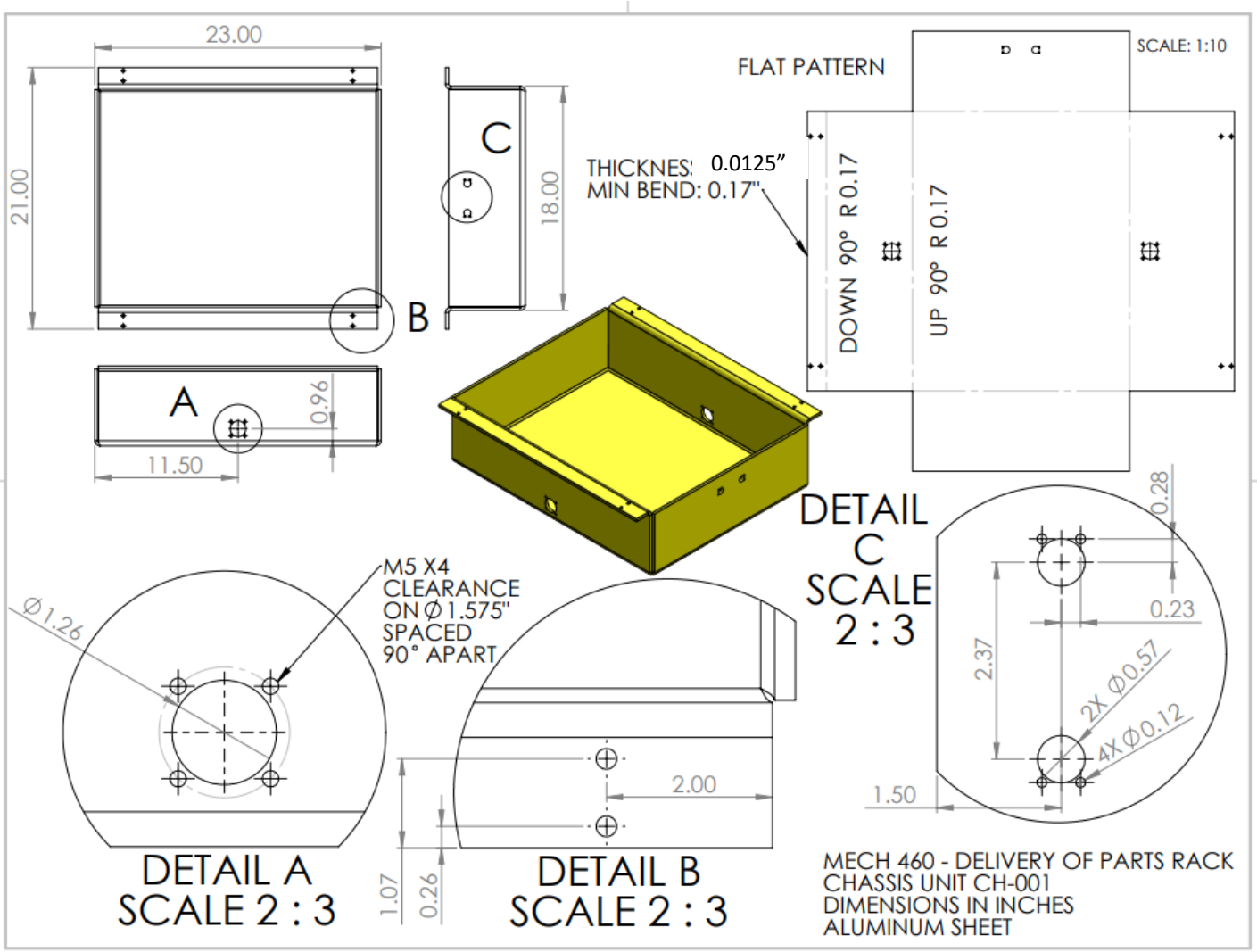

Figure 18: Detailed Drawing of Chassis

MECH 460 - DELIVERY OF PARTS RACK
CHASSIS UNIT ASSEMBLY
DIMENSIONS IN INCHES

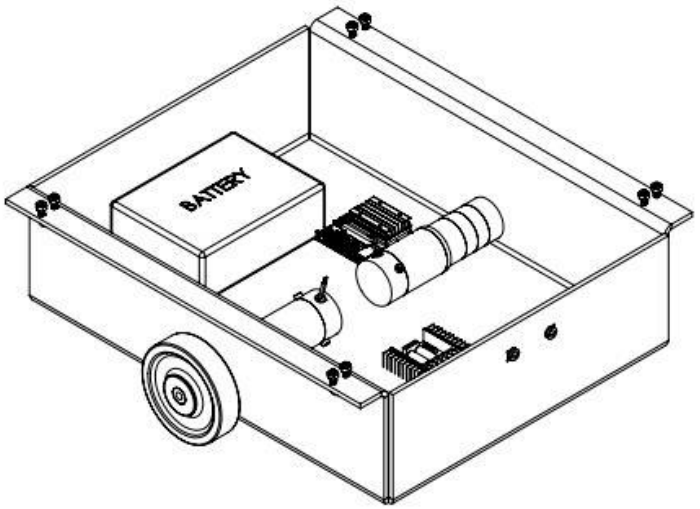

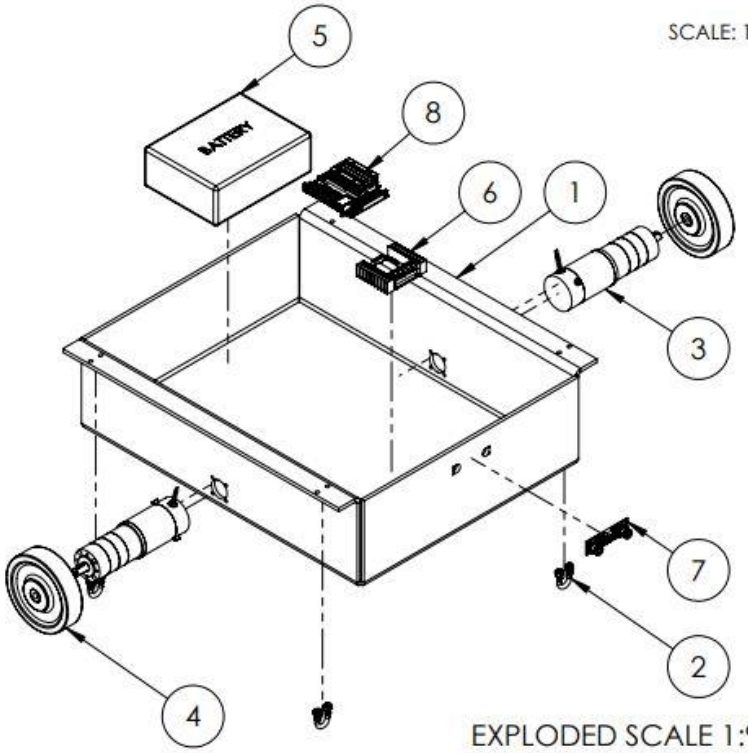

ITEM NO.	PART NUMBER	DESCRIPTION	QTY.
1	CH-001	1/4" Cut & Welded Aluminum Sheet Chassis	1
2	2936T31	Galvanized Steel U-Bolt	4
3	d22376gp2	Reversible DC GearMotor 24V	2
4	2328T78	Static-Control Rubber Wheel	2
5	Battery	24 V 35 AH Battery Pack	1
6	Sabertooth2x25A	Motor Controller	1
7	IMX219-36	Stereo Depth Camera	1
8	Jetson Nano	Controller Unit	1

Figure 19: Labeled Drawing of Chassis

Appendix B – Programming Workflow